JOURNAL OF NEUROSCIENCE METHODS

A novel technique for examining human brain activity associated with pedaling using fMRI

Jay P. Mehta [a,b], Matthew D. Verber [c], Jon A. Wieser [a], Brian D. Schmit [b], Sheila M. Schindler-Ivens [a,*]

[a] *Department of Physical Therapy, Marquette University, Milwaukee, WI 53201-1881, United States*
[b] *Department of Biomedical Engineering, Marquette University, Milwaukee, WI 53201-1881, United States*
[c] *Clinical and Translational Science Institute, Medical College of Wisconsin, Milwaukee, WI 53226, United States*

ABSTRACT

Advances in neural imaging technologies, such as functional magnetic resonance imaging (fMRI), have made it possible to obtain images of human brain activity during motor tasks. However, technical challenges have made it difficult to image the brain during multijoint lower limb movements like those involved in locomotion. We developed an MR compatible pedaling device and recorded human brain activity associated with rhythmic, alternating flexion and extension of the lower extremities. Ten volunteers pedaled at 30 RPM while recording fMRI signals in a GE 3T short bore MR scanner. We utilized a block design consisting of 3 runs of pedaling, each lasting 4 min. In a single run, subjects pedaled for 30 s and then rested for 30 s. This sequence was repeated 4 times. Conventional fMRI processing techniques, that correlate the entire BOLD signal with standard model, did not extract physiologically meaningful signal, likely due to magnetic field distortion caused by leg movement. Hence, we examined only the portion of the blood-oxygen-level dependent (BOLD) signal during movement-free periods. This technique takes advantage of the delayed nature of the BOLD signal and fits the falling portion of the signal after movement has stopped with a standard model. Using this approach, we observed physiologically plausible brain activity patterns associated with pedaling in the primary and secondary sensory and motor cortices and the cerebellum. To our knowledge, this is the first time that human brain activity associated with pedaling has been recorded with fMRI. This technique may be useful for advancing our understanding of supraspinal control of locomotor-like movements in health and disease.

© 2009 Elsevier B.V. All rights reserved.

1. Introduction

Recent advances in functional magnetic resonance imaging (fMRI) have made it possible to obtain high resolution images of human brain activity during motor tasks (Ciccarelli et al., 2005; Gordon et al., 1998; Rao et al., 1993, 1996a,b; Sahyoun et al., 2004). These and other neuroimaging technologies have led to a better understanding of how supraspinal structures contribute to movement in health and disease. However, technical challenges have made it difficult to use fMRI to image the human brain during multijoint movements of the lower extremities, particularly locomotion, which is one of the most important functions of the lower limbs. Hence, the goals of this study were to develop and validate a method for recording human brain activity with fMRI during a locomotor-like lower extremity task.

There are a number of challenges associated with using fMRI to image the brain during gross motor tasks of the lower extremities. Walking cannot be examined because of the need to remain supine and to keep the head still. Hence, an appropriate surrogate must be selected. Even if the head can be stabilized, large, multijoint movements of the lower extremities may distort the static magnetic field in the imaging environment making it difficult to record artifact-free blood-oxygen-level dependent (BOLD) signals during the actual movement portion of the task (Schenck, 1996). Moreover, any devices used for performing or recording movements during fMRI must be designed specially for the environment and constructed of materials with low magnetic susceptibility.

Because of these technical challenges, previous studies that have used fMRI to examine human brain activity during lower limb movement have employed single joint movement tasks and imagined locomotion. For example, several investigators have recorded functional images during ankle or knee flexion and extension (Ciccarelli et al., 2005; Dobkin et al., 2004; Jang et al., 2005; Luft et al., 2005; Sahyoun et al., 2004). Others have recorded whole brain activity during imagined walking and running (Jahn et al., 2004; Jahn et al., 2008). While some neural control strategies may be

shared across actual locomotion, imagined locomotion, and single joint movements of the lower limbs, it is unlikely that supraspinal control of each task is identical. Hence, in order to use fMRI to understand the role of the human brain in controlling the lower limbs, there is a need to develop techniques that record brain activity associated with activities that more closely resemble functionally relevant lower limb tasks.

In this paper we describe a novel technique for recording human brain activity associated with pedaling using fMRI. While pedaling is not the same as walking, it is a useful model of locomotion because it involves rhythmic, alternating extension and flexion of the both lower limbs and has been used extensively for studying normal and impaired locomotor control (Brown et al., 1997; Brown and Kautz, 1998, 1999; Kautz and Brown, 1998; Raasch et al., 1997; Raasch and Zajac, 1999). It is also possible to pedal a bicycle ergometer while lying supine on an MRI scanner bed and stabilizing the pelvis, trunk, and head. However, because traditional bicycle ergometers contain ferromagnetic components, it is not possible to use a standard ergometer in the imaging environment. Hence, we designed, fabricated, and validated an MR compatible pedaling device. We then developed an experimental set-up that minimized head movement and employed non-traditional signal processing techniques to extract physiologically meaningful fMRI signals associated with pedaling. Here, we describe the process through which these goals were achieved and present functional brain imaging data associated with human pedaling that were obtained with fMRI. Portions of these data have been presented in abstract (Wieser et al., 2008).

2. Materials and methods

In order to develop and test a new technique for estimating brain activity associated with locomotor-like movements, we conducted three fMRI experiments using a custom, instrumented pedaling device. Experiment 1 was designed to test the MR compatibility of the apparatus using a phantom. Experiment 2 was used to determine whether pedaling produces a measurable brain signal in humans when combined with a novel analysis approach designed to minimize motion artifacts. Experiment 3 was conducted to validate the analysis technique by applying it to finger and foot tapping movements.

2.1. Instrumentation

As shown in Fig. 1, the pedaling device designed for these experiments was a direct drive, bearing-free apparatus fabricated from non-metallic materials including polyvinyl chloride (PVC), Delrin, Phenolic, Nylon, and wood. A disc shaped flywheel was mounted on two solid vertical supports by way of a crankshaft. The crankshaft was made from Delrin, which is a self-lubricating plastic; thereby eliminating the need for bearings. The vertical supports were mounted on a base and secured with Nylon screws. The pedals were coupled to the crankshaft by way of crank arm that was adjustable in length to accommodate different body types. A pair of sandals was mounted on the pedals to secure the feet. The mechanical load on the pedaling device was created by friction between the crankshaft and the vertical supports. The device could be used to pedal forward or backward with speeds up to 80 RPM.

An MR compatible optical encoder (model TD 5207, Micronor Inc., CA) with resolution of 1.8° and ±100 RPM was used to measure crank position and velocity, although pedaling speed did not exceed 30 RPM in the present study. The encoder was enclosed in a housing, mounted on one of the vertical supports, and coupled to the crankshaft via a plastic chain and sprocket assembly arranged in a 1:1 ratio. Signals from the encoder were output via a

fiber optic cable to a controller unit (model MR 310, Micronor Inc., CA) located outside the scanner room. The controller converted the optical signals to electrical signals and produced analog outputs corresponding to crank position and velocity. Position and velocity data were sampled at 2000 Hz using a laptop computer with a 16 bit analog to digital converter and data acquisition software (micro 1401 mk II and Spike, Cambridge Electronics Design, UK). These data were used to compute mean pedaling velocity across subjects and trials.

A 3.0 T GE short bore MR scanner (General Electric Healthcare, Milwaukee, WI) and a GE single channel transmit/receive split head coil assembly (GE model 2376114) located at Froedtert Hospital in Milwaukee, WI was used for all experiments. Audacity (open source software) and Presentation (Neurobehavioral Systems, CA) software were used to deliver audio output to the subjects via MR compatible earphones (model SRM 212, Stax, Japan).

2.2. Experiment 1: MR compatibility of pedaling device

The purpose of the first experiment was to determine whether the pedaling device itself or movement of the device in the MR environment produced signal changes that resembled task-related brain activity. To this end, we conducted a series of experiments in which we recorded fMRI signals from a spherical, silicone head phantom (GE model 2359877) under different conditions. To examine the effects of our instruments on the fMRI signal, recordings were made with the phantom alone, the phantom and pedaling device, and the phantom, pedaling device, and electronics connected. There was also a condition in which an experimenter used a wooden stick (1.8 m) to pedal the device at a rate of 30 RPM while standing outside the 10 Gauss line. This condition was introduced to examine the effect of device motion on the MR signal. We reasoned that the experimenter and movement of his body outside the 10 G line would minimally affect the MR signal.

fMRI images were obtained using a gradient echo planar imaging (EPI) pulse sequence (36 contiguous slices in the sagittal plane; echo time (TE) = 25 ms, interscan period (TR) = 2 s, flip angle = 77°, field of view (FOV) = 24 cm, and 64 × 64 matrix). The resolution of the images was 3.75 mm × 3.75 mm × 4 mm. Raw fMRI data were converted to 3 dimensional (3D) images using Analysis of Functional NeuroImages (AFNI) software. The functional data were registered to the volume acquired halfway through the first run (50th TR) to compensate for any movement that may have occurred during or between data acquisition runs.

To estimate the effect of different conditions on the signal, we performed direct voxel-wise subtraction of each condition from the "phantom alone" condition, quantified the percent change in brightness between conditions, and calculated the signal to noise ratio for each condition per the following equation:

$$SNR = \frac{S}{0.655 \times SD_{noise}}$$

where SNR represents the signal to noise ratio, S is the mean value of the signal in a 36,000 μL area at the center of the phantom, and SD_{noise} is the average of the standard deviation of a 36,000 μL region outside the phantom. The scaling factor 0.655 was used to correct for changes in the distribution of Gaussian noise present in the raw dataset caused by calculation of the magnitude image from original complex MR data (Haacke et al., 1999).

2.3. Experiment 2: fMRI signals associated with pedaling

In this experiment we used an fMRI block design to determine the feasibility of recording physiological brain activity associated with pedaling. Each subject performed three runs of pedaling at a rate of 30 RPM. The pedaling rate of 30 RPM was selected because
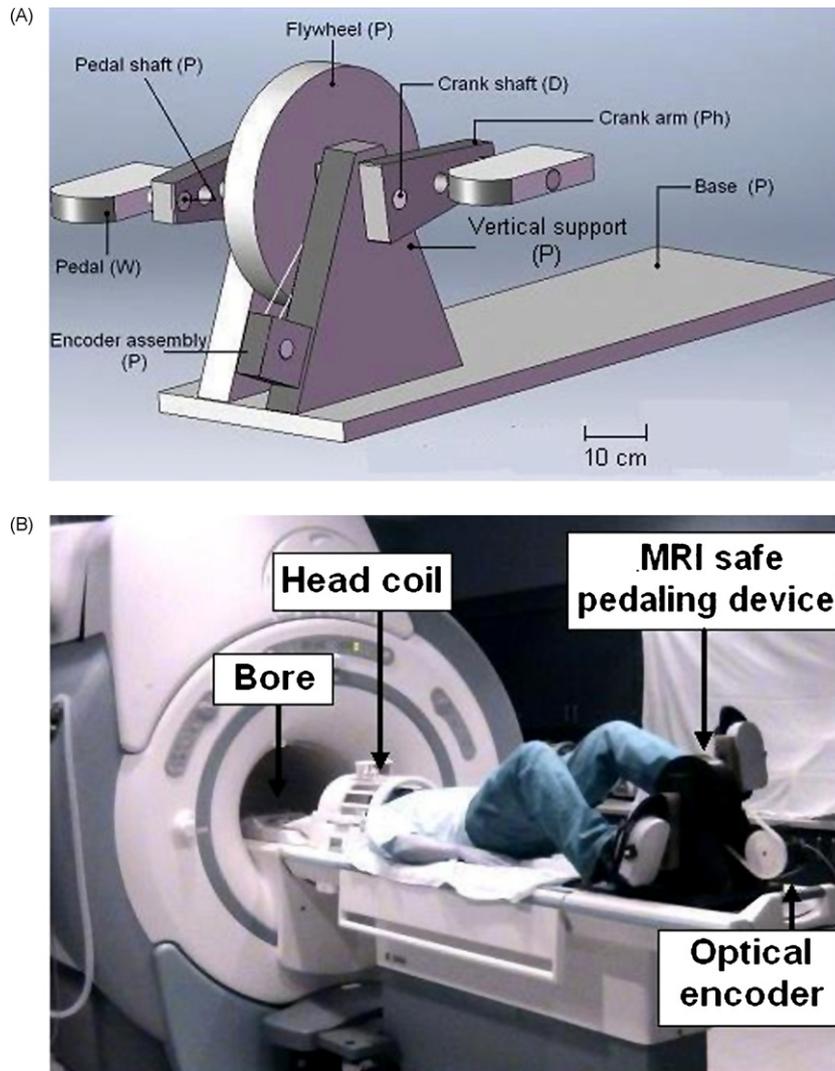
Fig. 1. (A) Diagram of MR compatible pedaling device. (B) Experimental set-up with subject positioned for pedaling. P: polyvinyl chloride, Ph: phenolic; W: wood, D: Delrin.

it is a relatively slow speed which was needed to minimize movement during pedaling; yet, it is fast enough to produce a natural, comfortable cadence. A single run consisted of 30 s of pedaling and 30 s of rest alternated 4 times.

Ten healthy individuals (6 males, mean age of 31 years, range: 21–53) volunteered for the study. Each subject gave written informed consent in accordance with institutional guidelines at Marquette University and the Medical College of Wisconsin and in accordance with the Declaration of Helsinki. Prior to participating, subjects were screened at least 3 times for MR safety. Subjects were excluded if they were pregnant, claustrophobic, obese, or had any implants or foreign bodies incompatible with fMRI. Subjects were also excluded if they had a history of any neurological impairments or physical conditions contraindicative to pedaling or exercise. Each subject participated in a familiarization session outside the MR environment where we explained the procedures and experimental protocol and taught subjects to pedal at a constant rate as indicated by a metronome. Because movement rate affects brain activity (Lutz et al., 2005; Agnew et al., 2004; Riecker et al., 2003; Rao et al., 1996a,b) we used a metronome to pace all the tasks to be sure that all volunteers moved at the same rate. During this session we also explained the importance of remaining still during fMRI scanning and encouraged subjects to keep their head and trunk stationary while pedaling.

During fMRI scanning, the subject lay supine on the scanner table with his or her feet positioned in the sandals and secured to the pedals (Fig. 1B). The subject's buttocks rested on the base of the pedaling device. The position of the pedaling device was adjusted until the subject was able to pedal comfortably and his or her legs did not touch the scanner. Each subject wore MR compatible earphones through which audio cues were delivered and an additional set of headphones to protect against scanner noise. The subject's head was placed in the head coil and adjusted to achieve symmetry in all 6 planes of movement (superior–inferior, left–right, anterior–posterior, roll, pitch, and yaw). To minimize head movement, the subject's head rested in a beaded vacuum pillow that enveloped the entire head (except the face) and created a firm, comfortable "brace" around the head. A chinstrap was used to prevent inferior–superior head movement, and additional foam padding was added as needed. The subject's torso was stabilized with a wide Velcro strap to minimize trunk movement. Additional padding under the buttocks and shoulders was provided for comfort. Subjects grasped an emergency squeeze ball that could be used at any time to signal a problem. Throughout the procedure, participants were monitored for safety and comfort and were able to communicate via intercom with the scanner technician.

Subjects were instructed to relax completely during rest periods. Throughout the experiment, subjects' pedaling performance

was monitored visually through the control room window and by examining the position and velocity data from the optical encoder. We also had access to real time information about head position. If the subject did not perform the task as instructed or if their head moved more than 2 mm, we reinstructed them and restarted the run.

EPI pulse sequence images were collected with TE = 25 ms, TR = 2 s, flip angle = 77°, FOV = 24 cm and matrix of 64 × 64. Thirty-six contiguous slices, each being 4 mm thick, were collected in the sagittal plane to cover the entire brain. Half way through the experimental protocol, 148 high resolution spoiled GRASS (gradient-recalled at steady state) anatomical images were also collected along the sagittal plane with TE = 3.9 ms, TR = 9.5 ms, flip angle = 12°, FOV = 24 cm, matrix of 256 × 244, and slice thickness of 1 mm.

As in the phantom study, 3D images were generated from the raw dataset. To minimize the effect of head movement between scans, all the functional datasets were registered to the functional scan that was obtained closest in time to the anatomical scan. Functional datasets were averaged across all runs to minimize the effect of noise. Correlation analysis was performed on the averaged data set.

Our first approach to processing pedaling-related fMRI signal used a conventional technique for block designs whereby the entire BOLD signal, including the portion of the signal concurrent with pedaling, was fit with a boxcar function. This approach produced an "activation" signal across the entire brain. Because it is physiologically improbable that the entire brain would be uniformly active during pedaling, we concluded that the BOLD signal may have been contaminated by movement artifact. We reasoned that movement of the legs during imaging distorted the static magnetic field and created an apparent change in the BOLD signal. Because lower

extremity movement occurred at the same time as pedaling, the apparent false BOLD signal was strongly correlated with the task.

To overcome this confound, we developed an approach to analyzing the data that minimized the effect of movement. Instead of correlating the entire BOLD signal (including the portion concurrent with pedaling) with the boxcar function, we extracted each 30 s period of data collected after pedaling stopped and correlated only this portion of the signal with the corresponding portion of the standard model (box car convolved with a gamma function). We refer to this as the "delayed" signal processing approach. Specifically, the model of the declining hemodynamic response was fit to each 30 s period of movement-free data. This model was obtained by convolving the boxcar with the gamma function, as would be done in the usual analysis, and then removing the pedaling periods in a similar manner as was used for the BOLD signal. From these data, we used AFNI to calculate the correlation between the model and the data and the percent change in BOLD signal from baseline. This approach is justified because the onset and termination of BOLD signals are delayed with respect to a given task (Bandettini and Cox, 2000; Blamire et al., 1992). Hence, movement-free BOLD signal should be present immediately after pedaling has stopped. The validity of this approach is further demonstrated in Fig. 2. In the frontal lobe (Fig. 2A), which is a brain region not expected to be associated with the task, there was a poor association between BOLD signal (shown in blue) and the trailing edge of the model (green). However, in the sensory and motor cortices (Fig. 2B) the post-movement portion of the BOLD signal declined in parallel with the falling edge of the model. Note that signals in both the frontal lobe and the sensorimotor cortex increased during the pedaling, consistent with the superposition of an artifact associated with leg motion onto the desired activity-related BOLD signal. The artifact itself appeared to resolve prior to the trailing edge of the hemodynamic model.
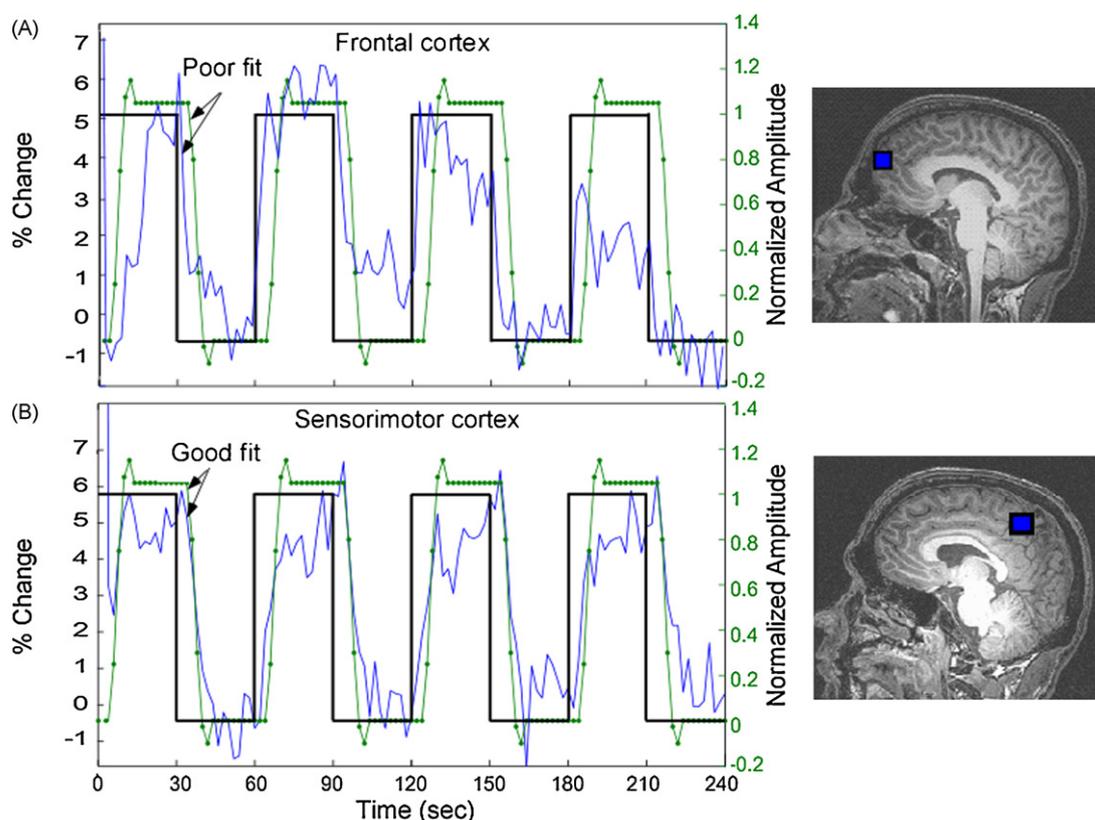
Fig. 2. Representative examples from a single subject of the relationship between the model and the BOLD signal. Time series voxels are from the frontal cortex (A) and sensorimotor cortex (B). The periods of pedaling and rest are shown in black. The BOLD signal is shown in blue, and the model is represented in green. The *x*-axis represents the number of TRs, where 1 TR = 2 s. Respectively, the left and right *y*-axes represent the amplitudes of the BOLD signal and the model in arbitrary units.

Table 1
Signal to noise ratio (SNR) across experimental conditions.

Condition	SNR
Phantom	232.2
Phantom + bike	230.7
Phantom + bike + electronics	232.9
Phantom + bike + electronics + movement	232.3

After overlaying the functional data on the anatomical images and identifying standard landmarks, data from each subject was transformed into the standardized coordinate system of Talairach and Tournoux (1988). Functional data were blurred using a 4 mm full width half maximum Gaussian filter, and then averaged across subjects to obtain a mean activity map. A group analysis was performed by entering individual subject data into a t-test to identify voxels containing BOLD signal that were significantly different from baseline. A threshold for the t-test was selected using a Monte Carlo simulation (AlphaSim) that set an appropriate individual voxel p-value and cluster size threshold to maintain a familywise error rate of $p < 0.05$. The locations of activated regions in the functional brain were determined from the Talairach atlas. The percent signal change in each activated region was quantified for each subject, individually. Values for percent signal change were computed by extracting voxels containing BOLD signal that was significantly correlated with the model. The threshold for a significant correlation was selected using a Monte Carlo simulation (AlphaSim) to set an individual voxel p-value to maintain a familywise error rate of $p < 0.05$. The mode of the percent signal change was calculated for each subject, and the group average of these values was calculated.

2.4. Experiment 3: validation of signal processing technique

The purpose of Experiment 3 was to validate the data processing technique used to identify brain activity associated with pedaling. Our goals were to demonstrate, in tasks with well described brain activations patterns and minimal movement, that (1) the delayed data processing approach provided the same results as the concurrent approach, and (2) that the delayed technique could detect similar activation patterns as have been previously published. Brain activation patterns as measured by fMRI are well described for unilateral finger and foot tapping (Ciccarelli et al., 2005; Rao et al., 1993,

1996a,b) where standard models are correlated with the entire BOLD signal. We reasoned that our approach could be validated by comparing tapping-related activation maps obtained with the delayed technique described here with those obtained from customary techniques that fit the entire BOLD signal with a standard model.

Using the parameters described for Experiment 2, we scanned the whole brain while subjects ($n = 7$) tapped their right index finger and then their right foot at rates of 4 and 2 Hz, respectively, timed using an auditory cue. We utilized a block design consisting of 16 s of tapping and 16 s of rest alternated 6 times. This movement sequence was performed one time each for the finger and the foot. Taps were recorded with custom-designed MR compatible switches to ensure that subjects performed the task as instructed.

3D images were generated from the raw dataset, and data were registered to the functional scan that was obtained closest in time to the anatomical scan. Data were processed using a conventional technique in which the entire BOLD response, including the portion concurrent with pedaling, was fit with a standard function and using the technique that examined only the portion of the BOLD signal after movement stopped (i.e. the delayed signal processing approach). Group mean activity maps and percent change in BOLD signal were computed as described above.

3. Results

3.1. Experiment 1: MR compatibility of pedaling device

The results of the phantom study suggested that the pedaling device, its electronics, and pedaling-like movement in the MR environment did not produce signal changes that were consistent with task-related brain activity. Fig. 3A and B shows the signals that were recorded from the phantom alone and from the phantom plus equipment and movement. Fig. 3C and D displays differences in signal brightness between conditions. When the device, electronics, and movement were introduced in a stepwise fashion, we saw a 0.2, 0.6, and 0.8% change in the average brightness, respectively. As shown in Fig. 3C, these changes were visually indiscernible when plotted on the same brightness scale as the signal recorded from the phantom alone. When the scale was adjusted to 5% of its original value (Fig. 3D), we observed

Table 2
Areas of activation with coordinates of center of mass for pedaling and tapping experiments.

Condition	Region[a]	Coordinates for center of mass			Volume (μL)
		R–L (mm)	A–P (mm)	I–S (mm)	
Pedaling	B. Primary Sensorimotor (1,2,3,4)	−1.1	36.2	59.6	9299
	B. SMA, Premotor (6)	−0.7	18.5	59.8	10708
	B. Cerebellar vermis (IV,V)	1.1	44.3	−9.7	6194
	B. Cerebellar Vermis (VIII)	2.5	60.0	−34.3	516
Finger tapping	L. Primary Sensorimotor (1,2,3,4)	40.4	27.0	46.5	10042
	R. Primary Sensorimotor (1,2,3,4)	−44.4	28.0	43.2	2948
	L. SMA, Premotor (6)	34.4	18.9	55.5	3636
	L. SMA, Premotor (6)	6.2	5.3	56.6	921
	R. SMA, Premotor (6)	−9.7	0.4	57.2	519
Foot tapping	L. Primary Sensorimotor (1,2,3,4)	0.87	37.2	58.0	10732
	R. Primary Sensorimotor (1,2,3,4)	−41.9	35.6	45.5	794
	L. Primary Sensorimotor (1,2,3,4)	51.0	25.3	36.2	634
	R. Primary Sensorimotor (1,2,3,4)	−25.4	14.9	27.2	469
	L. SMA, Premotor (6)	52.1	−0.9	37.3	319
	B. SMA, Premotor (6)	−1.9	15.8	59.9	5104
	R. Cerbellar vermis (IV,V)	−4.2	42.8	−9.6	1329
	L. Cerbellar vermis (Crus 1)	34.6	47.2	−27.9	229

R: Right, L: left, A: anterior, P: posterior, I: inferior, S: superior, B: bilateral, SMA: supplemental motor area. Negative values represent right, inferior, and anterior.

[a] Brain regions are described by name, Brodmann area (cortex), and cerebellar lobule (cerebellum).
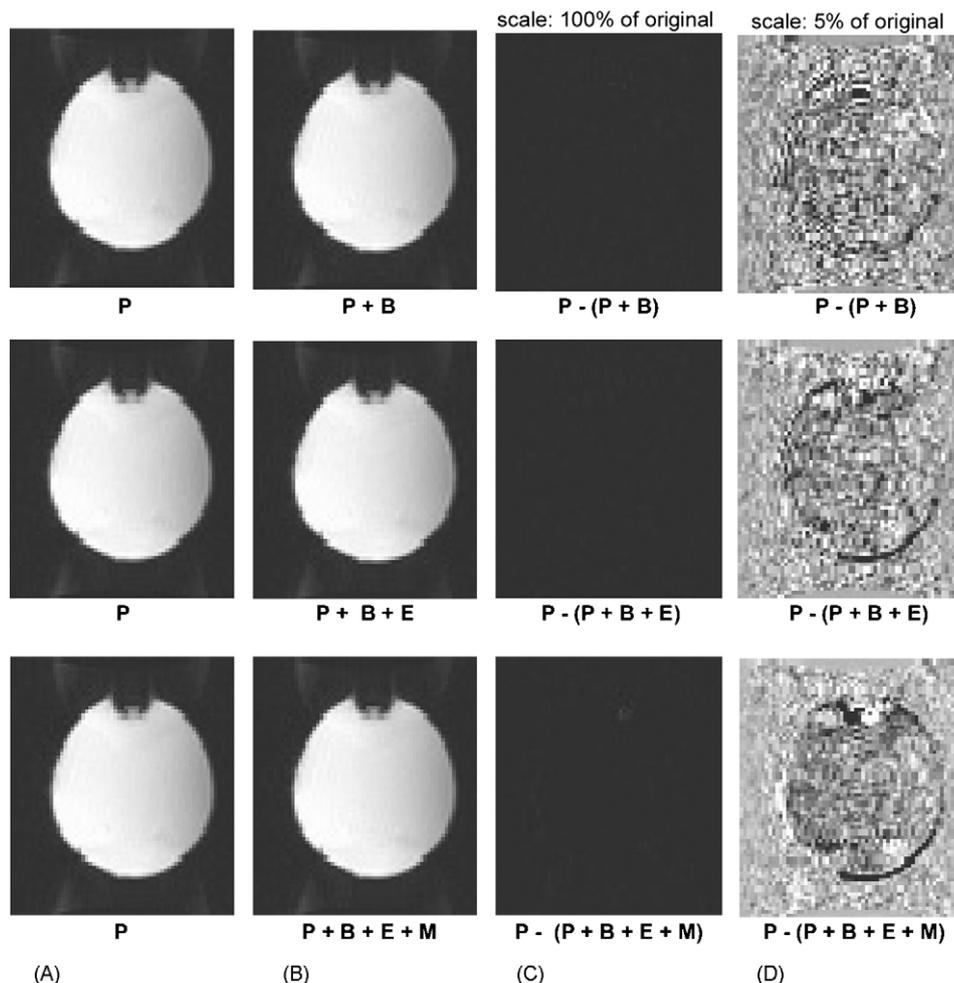
Fig. 3. Results of the phantom study. Images of the phantom alone (P) are shown in column A. Images of the phantom plus the pedaling device (B), electronics (E), and movement (M) are shown in column B. Columns C and D show the difference in signal between conditions on the original (C) and 5% of original (D) scale.

brightness changes around the edge of the phantom. There was a non-systematic spatial pattern of signal change within the phantom. Table 1 displays the signal to noise ratios for each condition. The addition of the device, electronics, and movement caused a 0.6%, 0.28%, and 0.02% change in the signal to noise ratio, respectively.

3.2. Experiment 2: fMRI signals associated with pedaling

All subjects were able to perform the pedaling task as evidenced by a group mean (SD) pedaling rate of 30.39 (0.38) RPM. On average, subjects displayed less than 1 mm of translational head movement and less than 1° of head rotation during pedaling. Group mean values for translational head movement were 0.28 (2.07), 0.06 (0.3) and 0.41 (0.51) mm in the superior–inferior, left–right and anterior–posterior directions respectively. On average, rotational movement was 0.15° (0.45), 0.03° (0.82) and 0.15° (0.35) in the roll, pitch, and yaw directions, respectively.

Pedaling was associated with bilateral activation of the primary sensory and motor cortices, the supplementary motor area, the premotor cortex, and the cerebellar vermis. Fig. 4 provides a pictorial representation of active brain regions for the entire group (left) and for a representative subject (right). Table 2 displays the spatial coordinates and volume of activation as measured from the group data. As shown in Table 3, the mode percent signal change associated with pedaling ranged from 0.55 to 2.75 with a mean (SD) value of 1.71 (0.67).

3.3. Experiment 3: validation of signal processing technique

As shown in Fig. 5, finger and foot tapping produced substantial activity in the primary sensory and motor cortices contralateral to the moving limb. Activity was more medially distributed during foot tapping as compared to finger tapping. We also observed bilateral activity in the premotor and supplemental motor areas during finger and foot tapping and activity in the cerebellar vermis during

Table 3
Mode percent change in BOLD signal during pedaling and tapping for individual subjects and group. Values for concurrent and delayed signal processing techniques are provided.

Subject	Pedaling	Finger tapping		Foot tapping	
	Delayed	Delayed	Concurrent	Delayed	Concurrent
1	1.51	–	–	–	–
2	2.54	1.42	1.42	1.83	1.83
3	0.55	–	–	–	–
4	1.92	–	–	–	–
5	2.75	1.12	2.04	1.65	1.30
6	2.02	1.63	1.35	2.32	1.34
7	1.51	1.39	1.34	1.13	1.18
8	0.94	1.10	0.70	1.01	0.88
9	1.52	0.94	0.71	1.00	0.70
10	1.85	1.02	1.31	1.01	1.11
Mean	1.71	1.23	1.22	1.42	1.19
SD	0.67	0.25	0.42	0.52	0.36
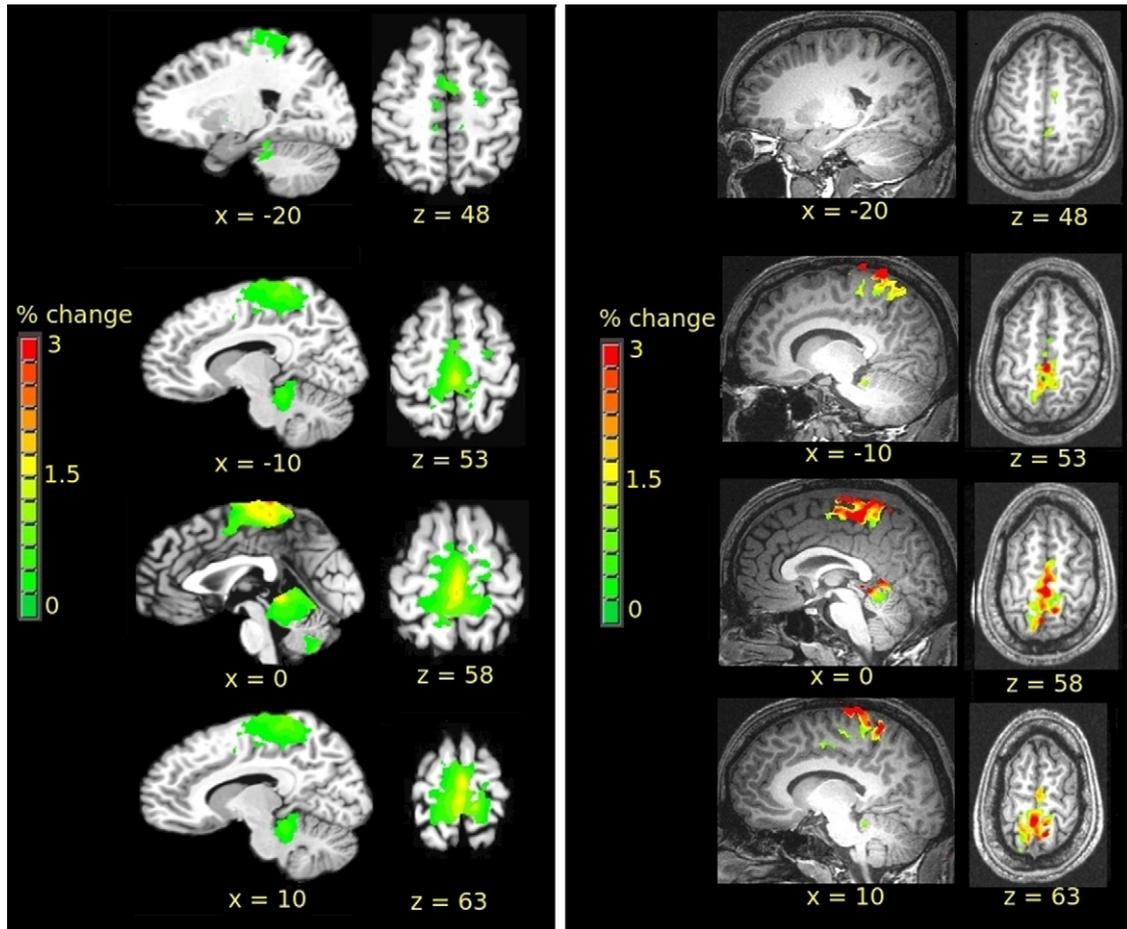
Fig. 4. Functional images overlayed on anatomical images for the entire group (left) and a representative subject (right). Images are slices taken from different sagittal and axial locations as specified by *x* and *z* coordinates. Color maps indicate percent change of the BOLD signal from baseline, with red indicating maximum percent change of the BOLD signal. *x*: left/right plane, *z*: superior/inferior plane, negative: right and inferior.
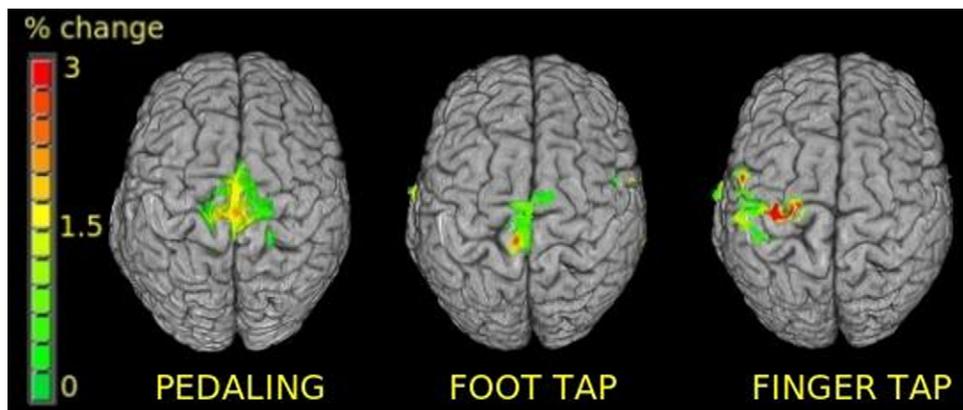
Fig. 5. Volume rendered functional images displaying cortical activity during pedaling (left), foot tapping (center) and finger tapping (right). Color maps indicate percent change in BOLD signal from baseline with red indicating maximum percent change in BOLD signal.

foot tapping. The mode percent signal change associated with finger and foot tapping ranged from 0.70 to 2.32 (see Table 3). Regardless of the technique (concurrent model versus delayed model), there was no significant difference in mode percent signal change measured during finger or foot tapping ($p > 0.15$).

4. Discussion

A novel technique for using fMRI to record human brain activity associated with pedaling was developed and tested in

this study. The technique uses a custom designed, MR compatible pedaling device and an unconventional (i.e. delayed) signal processing method that is capable of extracting BOLD signals associated with rhythmic, reciprocal, multijoint movement of the lower extremities. Using these methods we observed gray matter activity in the primary and secondary sensory and motor cortices of the brain and the cerebellum that was associated with pedaling. The results suggest that this approach would be useful for investigating brain contributions to locomotor control.

4.1. MR compatibility of pedaling device

Examining the MR compatibility of the pedaling device was essential because devices, particularly ferromagnetic objects, may induce changes in magnetic field homogeneity and cause image distortion (Schenck, 1996). We minimized this problem by constructing our device from non-metallic materials, which also ensured that it would not be drawn into the magnet where it could cause injury or equipment damage. We also used two well-established techniques for examining the effect of our device on image quality. First, we displayed and quantified differences in brightness between phantom images taken with and without the device and then we quantified the signal to noise ratio under the same conditions.

When differences in phantom images were displayed on the same scale as the original images, as is typically done for compatibility testing (Chinzei et al., 2000, 1999; Flueckiger et al., 2005; Izawa et al., 2006; Khanicheh et al., 2005), there were no visually detectable differences. However, when we rescaled the subtracted images to magnify differences, we saw brightness changes that were less than 1% of full-scale brightness and were arranged in a non-clustered fashion. These changes in the image would be difficult to interpret as task-related brain activity, which is typically clustered in specific brain regions. Note that these device-related changes were similar to others that have been considered acceptable. Many investigators do not alter the scale of the subtracted images or quantify brightness changes to identify small differences (Chinzei et al., 2000; Chinzei et al., 1999; Flueckiger et al., 2005; Gassert et al., 2006; Izawa et al., 2006; Khanicheh et al., 2005). Hence, it is likely that the amount of device-related signal change observed here was similar to that of other devices deemed compatible for MRI, although it is not possible to compare signal intensity changes because they were not reported in these previous studies. The MR compatibility of the device was further supported by changes in the signal to noise ratio across conditions that did not exceed 1% of the control condition. Previous studies have concluded that devices were MR compatible when equipment-related decreases in the signal to noise ratio were in the range of 1.8–7.95% (Chinzei et al., 2000; Chinzei et al., 1999; Gassert et al., 2006; Khanicheh et al., 2005; Suminski et al., 2007).

4.2. Head movement during pedaling

It was important to determine whether volunteers could pedal during fMRI without substantial head movement. If the head moved during imaging, the same portion of the brain might have appeared in a different voxel at different time points in the experiment. In this way, if movement was substantial, the functional image might have falsely displayed a change in the location or spatial extent of brain activity across tasks (Arnold et al., 2003; Field et al., 2000; Hajnal et al., 1994).

We observed less that 1 mm of head movement during pedaling. Others have suggested that small movements (<1 mm) are virtually impossible to prevent even under the most controlled circumstances (Field et al., 2000). Hence, the amount of head movement observed here was well within an acceptable range for fMRI and is comparable to that which has been deemed acceptable during other tasks involving considerably less movement of smaller body parts. Moreover, because the resolution of our images was 3.75 mm × 3.75 mm × 4 mm, the brain tissue in the center of any voxel would have remained in the same voxel despite movement. Hence, false signal detection in adjacent voxels should have been minimal.

Several factors may have helped minimize head movement during functional imaging, including subject comfort and the use of a beaded vacuum pillow, which made it nearly impossible to make large head movements. Moreover, volunteers were carefully instructed on the importance of remaining still during the experiment and practiced in a separate pre-scan session. Note that the instruction to remain still was a component of the motor control task and it is unclear how this component might have affected the measured brain activity. It may be useful in future studies to compare brain activity during actual and imagined pedaling where head movement should be negligible.

4.3. Validity of signal processing technique

Our data strongly suggest that the experimental paradigm and signal processing techniques extracted physiologically meaningful fMRI signals from the human brain that were associated with a continuous, bilateral lower extremity gross motor task. Several observations support this conclusion. Pedaling-related brain activity was observed in structures that are typically associated with movement such as the sensory and motor cortices and the cerebellum, but not in other areas of the brain. This observation occurred because the post-pedaling portion of BOLD signal that was used for analysis dropped gradually to baseline in sensorimotor structures. Hence, the signal was well correlated with our model. In contrast, the signals recorded from other portions of the brain such as the frontal lobe dropped abruptly after movement stopped (see Fig. 2). The gradually falling BOLD signals were likely caused by task-related brain activity, as it takes approximately 10 s for hemodynamic responses to return to baseline after a motor task (Bandettini and Cox, 2000). Conversely, rapidly declining BOLD signals were more likely caused by leg motion because they abated as soon as movement stopped. The fact that the gradually declining signals appeared in sensorimotor areas of the brain, and not across the entire brain, supports our conclusion that the patterns of brain activity observed were induced by brain activity associated with pedaling and not motion artifact.

The finger and foot tapping data further support the conclusion that our methods extracted physiologically meaningful brain activity associated with pedaling. When we analyzed the finger and foot tapping data using concurrent and delayed techniques, there was no difference in the spatial distribution of brain activity or the percent signal change. Moreover, the activation maps obtained with both processing techniques were comparable to those reported in the literature (Ciccarelli et al., 2005; Hayashi et al., 2008; Khushu et al., 2001; Rao et al., 1993, 1996a,b; Sahyoun et al., 2004). Most activation was observed in the contralateral primary and secondary sensory and motor cortices. Consistent with expected somatotopy, the spatial extent of activity migrated from lateral to medial portions of the primary sensory and motor cortices when subjects switched from finger to foot tapping.

The validity of our approach was further supported by the observation of brain activation patterns associated with pedaling that were similar to those recorded with other brain imaging techniques during pedaling and walking. Christensen et al. (2000) showed significant bilateral activation of the primary sensory and motor cortices, the supplemental motor area, and the anterior cerebellum using positron emission tomography (PET) to examine brain activation during pedaling. Using near-infrared spectroscopy, Miyai et al. (2001) have also detected substantial bilateral activity in the medial primary sensory and motor cortices and supplemental motor area during walking.

4.4. Supraspinal control of pedaling

While the focus of this study was to develop a technique for recording human brain activity associated with pedaling, the data obtain from the pedaling trials may shed some light on supraspinal control of rhythmic, reciprocal, lower extremity

flexion and extension tasks that are characteristic of locomotion. Consistent with previous literature (Christensen et al., 2000), we have shown that the primary sensory and motor cortices, premotor cortex, supplemental motor area, and cerebellum are involved in pedaling. However, the precise role of these structures remains unclear. Others have shown that passive pedaling (Christensen et al., 2000) and imagined walking (Jahn et al., 2004) produce similar brain activation patterns as actual pedaling and walking. It remains unclear whether the brain activity observed here was caused by the production of the pedaling behavior, the sensory feedback associated with pedaling, and/or the planning of the pedaling task. Moreover, a portion of the observed effects may have been due to the metronome. Some studies have shown that the cerebellum and premotor cortex are more active during externally cued as compared to self initiated movements (Taniwaki et al., 2006; Debaere et al., 2003). However, these effects are most robust when external cues occur at unpredictable intervals. In the present study, the cues occurred at predictable intervals which tend to produce brain activation patterns that share some characteristics with self initiated movements (Taniwaki et al., 2006; Jenkins et al., 2000). It is also unclear whether the pedaling-related brain activity observed here is unique to locomotion or if it is characteristic of any bilateral lower extremity task. Because the foot tapping task was performed unilaterally, this comparison cannot be made. Future studies will examine relationships among brain activity and various pedaling task demands, including passive and imagined pedaling and pedaling with and without auditory cues, to further elucidate the role of supraspinal structures in controlling this task. Finally, the application of these findings with respect to neural control of locomotion should be interpreted in light of limitations of the pedaling model. Pedaling is not the same as walking; it does not require balance or body weight support. Sensory cues associated with heel strike and toe off were not present during pedaling because the feet remained in constant contact with the pedals. As these components of the task may be important for supraspinal control of locomotion, a cautious interpretation of these finding with regard to walking is warranted.

5. Conclusion

This study demonstrates that fMRI can be used to record physiological activity from the human brain that is associated with pedaling. It further suggests that activity in the medial primary sensory and motor cortices, premotor cortex, supplementary motor area, and anterior cerebellum was associated with this task. Future studies will use this approach to further examine the role of supraspinal structures in producing locomotor-like movement in healthy and neurologically impaired individuals.

Acknowledgements

References

Agnew JA, Zeffiro TA, Eden GF. Left hemisphere specialization for the control of voluntary movement rate. Neuroimage 2004;22(1):289–303.

Arnold S, Ernst T, Tomasi D, Caparelli EC, Chang L. Residual effects of head movement in fMRI. In: Proceedings of the IEEE 29th annual northeast bioengineering conference; 2003. p. 77–8.

Bandettini PA, Cox RW. Event-related fMRI contrast when using constant interstimulus interval: theory and experiment. Magn Reson Med 2000;43:540–8.

Blamire AM, Ogawa S, Ugurbil K, Rothman D, McCarthy G, Ellermann JM, et al. Dynamic mapping of the human visual cortex by high-speed magnetic resonance imaging. Proc Natl Acad Sci U S A 1992;89(22):11069–73.

Brown DA, Kautz SA. Increased workload enhances force output during pedaling exercise in persons with poststroke hemiplegia. Stroke 1998;29(3):598–606.

Brown DA, Kautz SA. Speed-dependent reductions of force output in people with poststroke hemiparesis. Phys Ther 1999;79(10):919–30.

Brown DA, Kautz SA, Dairaghi CA. Muscle activity adapts to anti-gravity posture during pedalling in persons with post-stroke hemiplegia. Brain 1997;120(Pt 5):825–37.

Chinzei K, Hata N, Jolesz FA, Kikinis R. Surgical assist robot for the active navigation in the intraoperative MRI: Hardware design issues. In: Proceedings of the 2000 IEEE/RJ international conference on intelligent robots and systems, vol. 1; 2000. p. 727–32.

Chinzei K, Kikinis R, Jolesz FA. MR compatibility of mechatronic devices: Design criteria. In: Proceedings of the second international conference on medical image computing and computer-assisted intervention; 1999. p. 1020–31.

Christensen LO, Johannsen P, Sinkjaer T, Petersen N, Pyndt HS, Nielsen JB. Cerebral activation during bicycle movements in man. Exp Brain Res 2000;135(1):66–72.

Ciccarelli O, Toosy AT, Marsden JF, Wheeler-Kingshott CM, Sahyoun C, Matthews PM, et al. Identifying brain regions for integrative sensorimotor processing with ankle movements. Exp Brain Res 2005;166:31–42.

Debaere F, Wenderoth N, Sunaert S, Van Hecke P, Swinnen SP. Internal vs external generation of movements: differential neural pathways involved in bimanual coordination performed in the presence or absence of augmented visual feedback. Neuroimage 2003;19:764–76.

Dobkin BH, Firestine A, West M, Saremi K, Woods R. Ankle dorsiflexion as an fMRI paradigm to assay motor control for walking during rehabilitation. Neuroimage 2004;23(1):370–81.

Field AS, Yen YF, Burdette JH, Elster AD. False cerebral activation on BOLD functional MR images: study of low-amplitude motion weakly correlated to stimulus. Am J Neuroradiol 2000;21:1388–96.

Flueckiger M, Bullo M, Chapuis D, Gassert R, Perriard Y. fMRI compatible haptic interface actuated with traveling wave ultrasonic motor. In: 2005 IEEE industry applications conference; 2005. p. 2075–82.

Gassert R, Moser R, Burdet E, Bleuler H. MRI/fMRI-compatible robotic system with force feedback for interaction with human motion. IEEE/ASME Trans Mechatronics 2006;11(2):216–24.

Gordon AM, Lee JH, Flament D, Ugurbil K, Ebner TJ. Functional magnetic resonance imaging of motor, sensory, and posterior parietal cortical areas during performance of sequential typing movements. Exp Brain Res 1998;121:153–66.

Haacke EM, Brown RW, Thompson MR, Venkatesan R. Magnetic resonance imaging: physical principles and sequence design. New York: Wiley; 1999.

Hajnal JV, Myers R, Oatridge A, Schwieso JE, Young IR, Bydder GM. Artifacts due to stimulus correlated motion in functional imaging of the brain. Magn Reson Med 1994;31:283–91.

Hayashi MJ, Saito DN, Aramaki Y, Asai T, Fujibayashi Y, Sadato N. Hemispheric asymmetry of frequency-dependent suppression in the ipsilateral primary motor cortex during finger movement: a functional magnetic resonance imaging study. Cereb Cortex 2008;18:2932–40.

Izawa J, Shimizu H, Gomi H, Toyama S, Ito K. MR compatible manipulandum with ultrasonic motor for fMRI studies. In: Proceedings of the 2006 IEEE international conference on robotics and automation; 2006. p. 3850–4.

Jahn K, Deutschlander A, Stephan T, Kalla R, Wiesmann M, Strupp M, et al. Imaging human supraspinal locomotor centers in brainstem and cerebellum. Neuroimage 2008;39(2):786–92.

Jahn K, Deutschlander A, Stephan T, Strupp M, Wiesmann M, Brandt T. Brain activation patterns during imagined stance and locomotion in functional magnetic resonance imaging. NeuroImage 2004;22(4):1722–31.

Jang SH, You SH, Kwon YH, Hallett M, Lee MY, Ahn SH. Cortical reorganization associated lower extremity motor recovery as evidenced by functional MRI and diffusion tensor tractography in a stroke patient. Restor Neurol Neurosci 2005;23(5–6):325–9.

Jenkins IH, Jahanshahi M, Jueptner M, Passingham RE, Brooks DJ. Self-initiated versus externally triggered movements. II. The effect of movement predictability on regional cerebral blood flow. Brain 2000;123(Pt 6):1216–28.

Kautz SA, Brown DA. Relationships between timing of muscle excitation and impaired motor performance during cyclical lower extremity movement in post-stroke hemiplegia. Brain 1998;121(Pt 3):515–26.

Khaniceh A, Muto A, Trantafyllou C, Weinberg B, Astrakas L, Tzika A, et al. MR compatible ERF driven hand rehabilitation device. In: Proceedings of the 2005 IEEE 9th international conference on rehabilation robotics; 2005.

Khushu S, Kumaran SS, Tripathi RP, Gupta A, Jain PC, Jain V. Functional magnetic resonance imaging of the primary motor cortex in humans: response to increased functional demands. J Biosci 2001;26(2):205–15.

Luft AR, Forrester L, Macko RF, McCombe-Waller S, Whitall J, Villagra F, et al. Brain activation of lower extremity movement in chronically impaired stroke survivors. Neuroimage 2005;26(1):184–94.

Lutz K, Koeneke S, Wustenberg T, Jancke L. Asymmetry of cortical activation during maximum and convenient tapping speed. Neurosci Lett 2005;373(1):61–6.

Miyai I, Tanabe HC, Sase I, Eda H, Oda I, Konishi I, et al. Cortical mapping of gait in humans: a near-infrared spectroscopic topography study. Neuroimage 2001;14(5):1186–92.

Raasch CC, Zajac FE. Locomotor strategy for pedaling: muscle groups and biomechanical functions. J Neurophysiol 1999;82(2):515–25.

Raasch CC, Zajac FE, Ma B, Levine WS. Muscle coordination of maximum-speed pedaling. J Biomech 1997;30(6):595–602.

Rao SM, Bandettini PA, Binder JR, Bobholz JA, Hammeke TA, Stein EA, et al. Relationship between finger movement rate and functional magnetic resonance signal change in human primary motor cortex. J Cereb Blood Flow Metab 1996a;16(6):1250–4.

Rao SM, Binder JR, Bandettini PA, Hammeke TA, Yetkin FZ, Jesmanowicz A, et al. Functional magnetic resonance imaging of complex human movements. Neurology 1993;43(11):2311–8.

Rao SM, Bandettini PA, Binder JR, Bobholz JA, Hammeke TA, Stein EA, et al. Relationship between finger movement rate and functional magnetic resonance signal change in human primary motor cortex. J Cereb Blood Flow Metab 1996b;16:1250–4.

Riecker A, Wildgruber D, Mathiak K, Grodd W, Ackermann H. Parametric analysis of rate-dependent hemodynamic response functions of cortical and subcortical brain structures during auditorily cued finger tapping: a fMRI study. Neuroimage 2003;18(3):731–9.

Sahyoun C, Floyer-Lea A, Johansen-Berg H, Matthews PM. Towards an understanding of gait control: brain activation during the anticipation, preparation and execution of foot movements. Neuroimage 2004;21(2):568–75.

Schenck F. The role of magnetic susceptibility in magnetic resonance imaging: MRI magnetic compatibility of the first and second kinds. Med Phys 1996;23(6):815–50.

Suminski A, Zimbelman J, Scheidt R. Design and validation of a MR-compatible pneumatic manipulandum. J Neurosci Methods 2007;163:255–66.

Talairach J, Tournoux P. Co-planar stereotaxic atlas of the human brain: 3-dimensional proportional system—an approach to cerebral imaging. New York: Thieme Medical Publishers; 1988.

Taniwaki T, Okayama A, Yoshiura T, Togao O, Nakamura Y, Yamasaki T, et al. Functional network of the basal ganglia and cerebellar motor loops in vivo: different activation patterns between self-initiated and externally triggered movements. Neuroimage 2006;31:745–53.

Wieser J, Mehta J, Schmit BD, Verber M, Schindler-Ivens SM. A novel technique for examining human brain activity during locomotion using fMRI. Society for Neuroscience; 2008.